Supplemental Materials

Molecular Biology of the Cell

Stoddard et al.

Supplemental Information for

Tetrahymena RIB72A and RIB72B are Microtubule Inner Proteins in the ciliary doublet microtubules

Daniel Stoddard[1,2], Ying Zhao[3,†], Brian A. Bayless[4], Long Gui[2], Panagiota Louka[5], Drashti Dave[5], Swati Suryawanshi[5], Raphaël F.-X. Tomasi [6], Pascale Dupuis-Williams[7,8], Charles N. Baroud[6,9] , Jacek Gaertig[5,*], Mark Winey[3,4,*], Daniela Nicastro[1,2,*]

1) Department of Biology, Rosenstiel Basic Medical Sciences Research Center, Brandeis University, Waltham, MA 02453, USA
2) Departments of Cell Biology and Biophysics, University of Texas Southwestern Medical Center, Dallas, TX 75390, USA
3) Department of Molecular, Cellular & Developmental Biology University of Colorado Boulder, Boulder, Colorado 80309, USA
4) Department of Molecular and Cellular Biology, University of California, Davis, CA, 95616, USA
5) Department of Cellular Biology, University of Georgia, Athens, GA, 30602, USA
6) Department of Mechanics, LadHyX, CNRS and Ecole Polytechnique, 91128 Palaiseau Cedex, France
7) UMR-S 1174 Inserm, Universite Paris-Sud, Bat 443, 91405 Orsay Cedex, France
8) e Ecole Supérieure de Physique et de Chimie Industrielles ParisTech, 10 rue Vauquelin, 75005 Paris, France
9) Institut Pasteur, Physical Microfluidics and Bioengineering, Department of Genomes and Genetics, 25-28 Rue du Dr. Roux, 75015 Paris, France

[†]) current address:
Ying Zhao, Department of Chemistry and Biochemistry, University of California, San Diego, CA, 92093, USA

*Corresponding Authors: Daniela Nicastro, Departments of Cell Biology and Biophysics, University of Texas Southwestern Medical Center, Dallas, TX 75390, USA; Phone: (++1) 214 648 3925; Fax: (++1) 214 648 7491; E-mail: daniela.nicastro@utsouthwestern.edu;
Mark Winey, Department of Molecular and Cellular Biology, University of California, Davis, CA, 95616, USA; Phone +1 530 752-6778; Fax +1 530 752-2604; E-mail: mwiney@ucdavis.edu; Jacek Gaertig, Department of Cellular Biology, University of Georgia, Athens, GA 30602, USA, phone 706 542 3409; email: jgaertig@uga.edu.

Supplementary Table 1. Strains used in this study and image processing information where applicable

Name	Strain	LM only	Cryo-ET: # of tomograms included	Averaged repeats	Resolution[a] (nm)	Used in Figure(s)
WT[b]	CU428		7	500	3.4	3-8, S1,S3,S4
RIB72A-KO	*RIB72A-KO*		5	758	4.4	3-7[c], S1[d],S4
RIB72B-KO	*RIB72B-KO*		5	702	4.4	3-7, S1,S4
RIB72A/B-KO	*RIB72A/B-KO*		5	699	4.4	3-7 S1,S3,S4
RIB72B-GFP	*RIB72B-KO: RIB72B-GFP*		5	735	4.6	8
RIB72A-mCherry, GFP-CEN1	RIB72A-mCherry, GFP-CEN1	X				2
RIB72A-mCherry, GFP-ATU	RIB72A-mCherry, GFP-ATU	X				2
RIB72B-mCherry, GFP-RIB72A	RIB72B-mCherry, GFP-RIB72A	X				2
GFP-RIB72A	*RIB72B-KO: GFP-RIB72A*	X				S1
RIB72B-mCherry	*RIB72A-KO: RIB72B-mCherry*	X				S1

[a]The 0.5 Fourier shell correlation criterion was used to estimate the resolution of the averaged repeats at the site of the doublet microtubule.
[b]WT includes previous published data (Vasudevan, Song et al. 2015).
[c] *RIB72A-KO* generated by Winey Lab
[d] *RIB72A-KO* generated by Gaertig lab

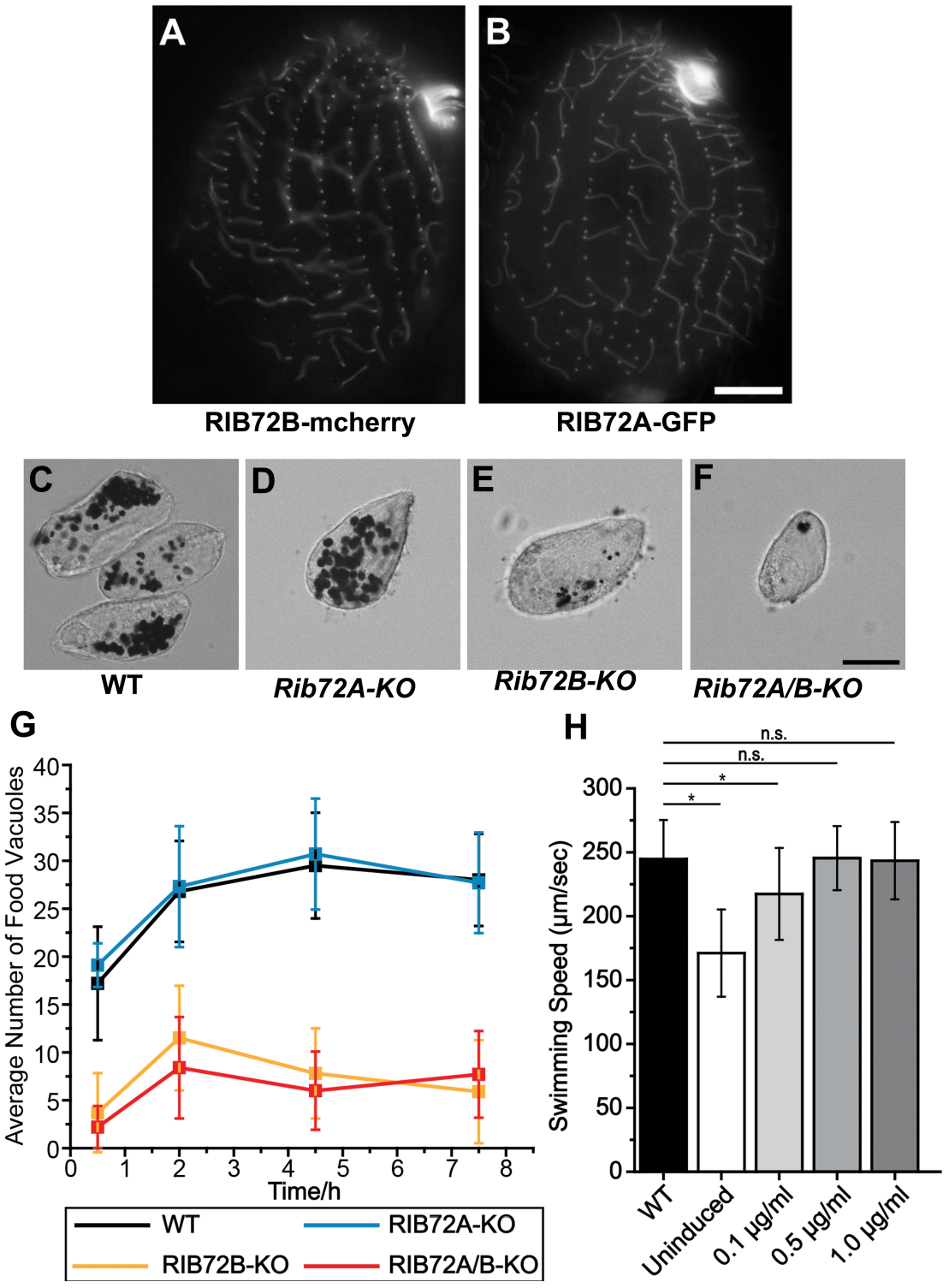

Figure S1. RIB72A and RIB72B localize independently of each other to cilia and basal bodies. (A, B) Fluorescent light microscopy images of fixed *Tetrahymena* cells shows (A) GFP-

tagged RIB72A in the *RIB72B-KO* mutant background, and (B) RIB72B-mCherry in the *RIB72A-KO* mutant background still localizing to cilia and basal bodies. Scale bars: 10 μm. **(C-F)** Phase contrast images of fixed *Tetrahymena* cells from WT (C), *RIB72A-KO* (D), *RIB72B-KO* (E) and *RIB72A/B-KO* (F) showing phagocytic vacuoles stained with India ink that was provided in the growth medium. Scale bar: 20 μm. **(G)** The number of phagocytic vacuoles was recorded at different time points after addition of the India ink. The most severe phagocytosis defects were evident in *RIB72B-KO* (E) and *RIB72A/B-KO* (F). (H) The expression level of RIB72B-GFP is induced by different levels of cadmium. Error bars represent standard deviations and asterisks indicate statistical significance at $p<0.01$ (one way ANOVA); n.s., non-significant, $p>0.05$.

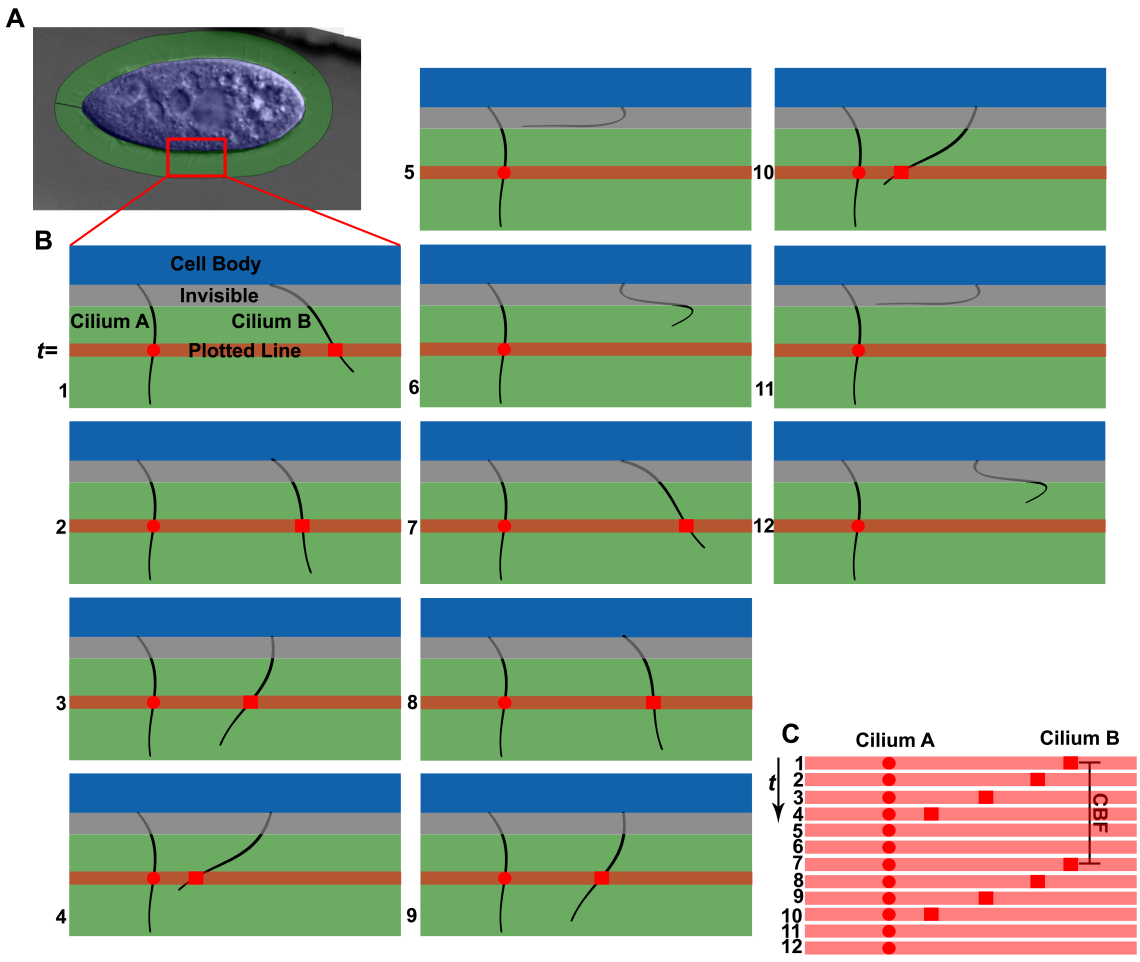

Figure S2. Schematic drawings explaining the generation of chronographs based on high-speed video imaging (shown in Figure 4). (A) First frame of a video was used to mark the cell body (blue) and cilia regions (green) of a swimming *Tetrahymena* cell. The red box outlines an area in the cell periphery that is shown at higher zoom in (B). **(B)** Selected area of the cell periphery of a swimming *Tetrahymena* cell at different time-points t=1-12 in chronological order. Two cilia are drawn: cilium A is stalled, whereas cilium B undergoes two complete beating cycles between t=1 and t=12. Note that beating cilia are not visible during their recovery stroke (e.g. cilium B at time-points 5,6 and 11,12), because the cilium is moving too close to the cell body and

“disappears” in the fringe close to the cell caused by DIC imaging. The red lines show the position which was plotted over time to produce the chronograph seen in (C); note the red circle and squares on the red line that indicate where the line transects a cilium. **(C)** Chronograph of cilia A and B constructed from lines that transect the video frames at the same location over time. Cilium A is stalled and does not change position throughout the Chronograph as indicated by the vertical column of circles. Cilium B is actively beating and changes position over time t as indicated by the red squares. The cilia beat frequency (CBF) is the time required for one complete beating cycle including the recovery stroke.

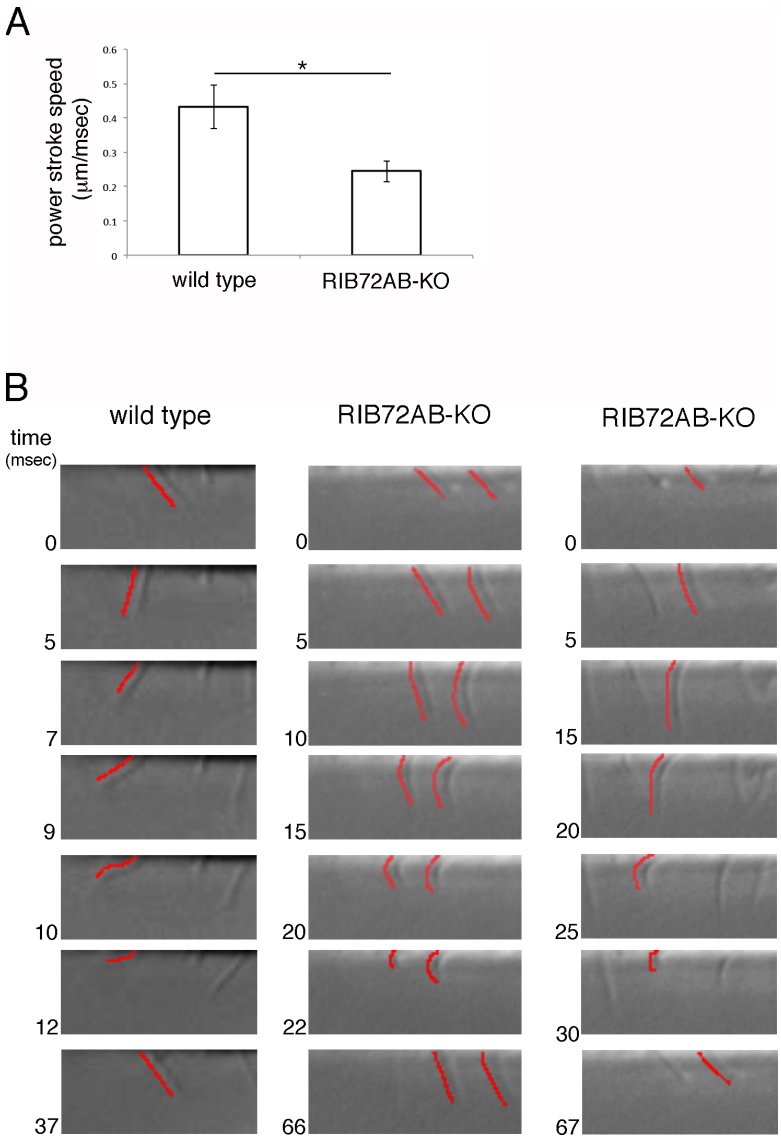

Figure S3. ***RIB72A/B-KO*** **cilia have a slower power stroke and waveform defects. (A)** A graph showing the power stroke speed values in wild-type (0.43 µm/msec, n cilia = 10, n cells =3) and *RIB72A/B-KO* (0.24 µm/msec n cilia = 10, n cells =3) cilia. The values were extracted from the chronographs (Figure 1B-E); the inverse slope of a short diagonal line of a cilium trace represents the speed of the power stroke. Error bars represent standard deviation and asterisk shows statistical significance at $p < 0.001$ (t-test). **(B)** Successive frames showing examples of individual cilia obtained from wild-type and *RIB72A/B-KO* extracted cilia videos (video S1, video S4). The red

line in each frame traces the shape of the same cilium. Note that cilia are invisible in most of the recovery stroke as their shafts lie close to the cell surface.

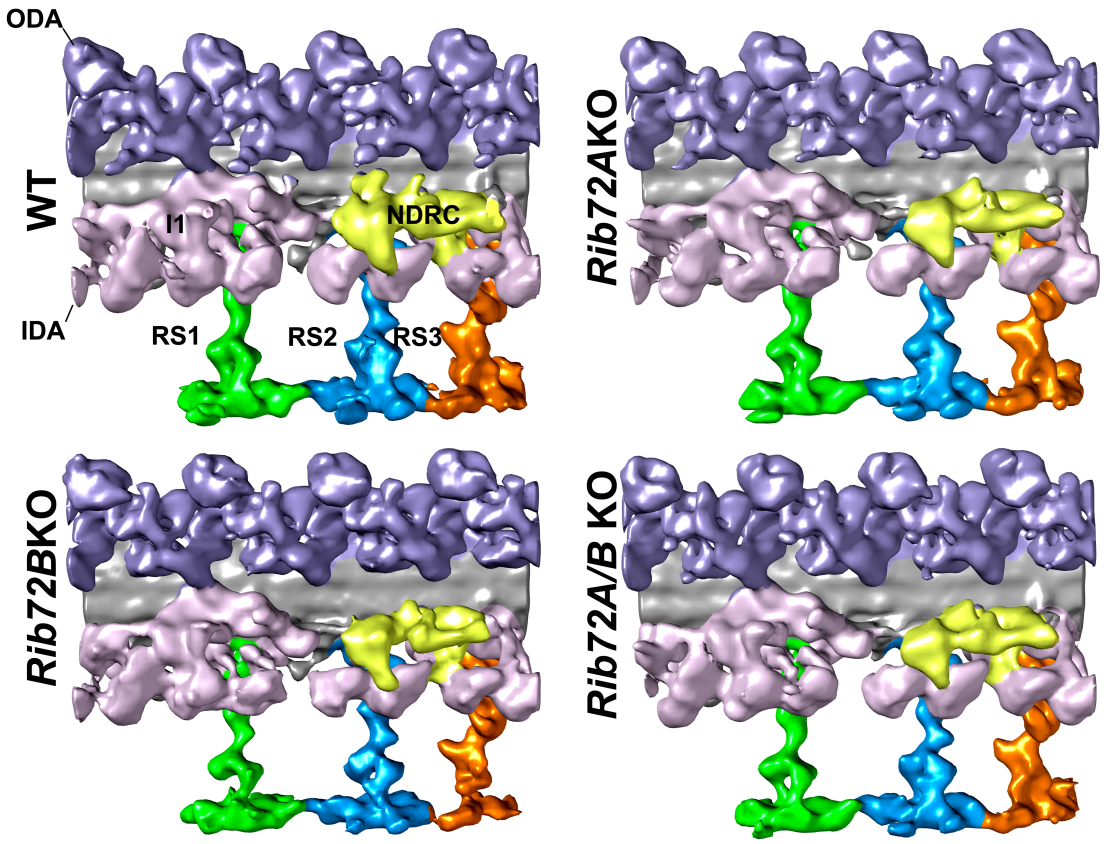

Figure S4. All axonemal structures associated to the outside of the DMTs appeared unchanged in the mutants. **(A-D)** Isosurface renderings in longitudinal front view (proximal on the left) of *Tetrahymena* axonemal repeat units of WT (A), *RIB72A-KO* (B), *RIB72B-KO* (C), and the double mutant (D). Colors: Inner dynein arms IDA (rose); nexin dynein regulatory complex N-DRC (yellow); outer dynein arms ODA (lavender), radial spokes 1 (green) 2 (blue) 3 (orange).

Supplemental Video Legends:

Video S1. A wild-type *Tetrahymena* cell swimming inside a microfluidic channel, recorded at 2000 frames/sec. (Stills appear in Figure 4 and Figure S3)

Video S2. A *Tetrahymena RIB72A-KO* cell swimming inside a microfluidic channel, recorded at 2000 frames/sec. (Stills appear in Figure 4)

Video S3. A *Tetrahymena RIB72B-KO* cell swimming inside a microfluidic channel, recorded at 2000 frames/sec. (Stills appear in Figure 4)

Video S4. A *Tetrahymena RIB72A/B-KO* cell swimming inside a microfluidic channel, recorded at 2000 frames/sec. (Stills appear in Figure 4 and Figure S3)

Video S5. A *Tetrahymena RIB72A/B-KO* cell swimming inside a microfluidic channel, recorded at 2000 frames/sec. Red arrow marks a cilium with a kink near the distal region.